EUROPEAN ORGANIZATION FOR NUCLEAR RESEARCH

May 15, 2017

D-hadron correlations in p-Pb collisions at $\sqrt{s_{\rm NN}}$ = 5.02 TeV

Authors list to be filled

Abstract

In this note, we present the analysis of azimuthal correlations of D mesons and primary charged particles performed in the ALICE central barrel in p-Pb collisions at $\sqrt{s_{NN}}$ = 5.02 TeV. After a description of the analysis strategy, corrections and systematic uncertainties, the results obtained for prompt D^0, D^{*+} and D^+mesons in different ranges of transverse momentum of the D meson and of the associated particles are presented and compared to Monte Carlo models.

Contents

1 Introduction and Motivation

The study of the azimuthal correlations of heavy-flavoured particles and charged particles at the LHC energies provides a way to characterize charm production and fragmentation processes in pp collisions as well as a way to probe our understanding of QCD in the perturbative regime, accessible in a large kinematic range given the large mass of heavy quarks. Flavour conservation in QCD implies that charm quarks are always produced as pairs of quarks and anti-quarks. The azimuthal correlations obtained using a meson carrying a heavy quark as trigger particle with the other charged particles in the same event give the possibility to study the underlying charm production mechanism in detail. In particular, prompt charm quark-antiquark pair production leads back to back in azimuth at first order in leading-order perturbative-QCD (pQCD). Heavy quarks produced from the splitting of a massless gluon can be rather collimated and may generate sprays of hadrons at small $\Delta\phi$. Finally, for hard-scattering topologies classified as "flavour-excitation", a charm quark undergoes a hard interaction from an initial splitting ($g \rightarrow c\bar{c}$), leading to a big separation in rapidity of the hadrons originating from the antiquark (quark) with respect to the trigger D meson and contribute to a rather flat term to the $\Delta\phi$-correlation distribution.

Heavy-flavour correlation studies in more complex collisional systems, like Pb-Pb, play a crucial role in studying the modification of the fragmentation of charmed jets due to in-medium (or cold nuclear matter, in case of p-Pb collisions) effects, in a similar way as it was done for di-hadron correlation studies in heavy-ion collisions (see for example [4, 5]). Furthermore, the recent observation of long range correlations in p-Pb for light flavour hadrons and for heavy-flavour decay electrons [1] points to possible collective effects or effects originating from gluon saturation in the initial state. More information could be extracted by the eventual observation of the same effect with D mesons.

In the following, we describe the analysis strategy for p-Pb in all its steps, and we describe the list of corrections and the estimation of the systematic uncertainties done. After a section dedicated to detailed studies performed with Monte Carlo simulations to check the different analysis steps, we present the results of $\Delta\phi$ correlations obtained for prompt D^0, D^+ and D^{*+} in different ranges of transverse momentum for the D-meson (trigger particle) and the associated particles.

2 Data sample

The list of runs used for the analysis, for each of the data taking periods is listed in table 1:

Type	**Production**	**Run list**	**nEvents**
Monte-Carlo	LHC17d2a, fast/AOD	265525, 265521, 265501, 265500, 265499, 265435, 265427, 265426, 265425, 265424, 265422, 265421, 265420, 265419, 265388, 265387, 265385, 265384, 265383, 265381, 265378, 265377, 265344, 265343, 265342, 265339, 265338, 265336, 265335, 265334, 265332, 265309, 267165, 267164, 267163, 267166 = **[22 runs]**	??M
Data	"LHC16q, pass1_CENT_woSDD/AOD"	265525, 265521, 265501, 265500, 265499, 265435, 265427, 265426, 265425, 265424, 265422, 265421, 265420, 265419, 265388, 265387, 265385, 265384, 265383, 265381, 265378, 265377, 265344, 265343, 265342, 265339, 265338, 265336, 265335, 265334, 265332, 265309 = **[32 runs]**	261M total
	"LHC16q, pass1_FAST/AOD"	265525, 265521, 265501, 265500, 265499, 265435, 265427, 265426, 265425, 265424, 265422, 265421, 265420, 265419, 265388, 265387, 265385, 265384, 265383, 265381, 265378, 265377, 265344, 265343, 265342, 265339, 265338, 265336, 265335, 265334, 265332, 265309 = **[32 runs]**	260M
	"LHC16t, pass1_CENT_wSDD/AOD"	267166, 267165, 267164, 267163 = **[4 runs]**	40M
	"LHC16t, pass1_FAST/AOD"	267166, 267165, 267164, 267163 = **[4 runs]**	41M

Table 1: Data Set and Run list

3 Analysis strategy

The analysis strategy follows the one used fro 2013 p-Pb data sample. The particle pairs are formed by trigger particles defined by the transverse momentum threshold $p_{\rm T} > p_{\rm T}^{\rm trig}$ and associated particles defined by $p_{\rm T} > p_T^{\rm assoc}$. Each pair of particles is considered only once by requiring $p_{\rm T}^{\rm assoc} < p_{\rm T}^{\rm trigg}$. In D meson correlations, the particle identification defines the trigger particle rather than a momentum cut and therefore the momentum range of the associated particles is not constrained by that of the trigger particle. Our definition of associated particle includes any charged particle coming from the primary vertex of interaction, including those coming from strong and electromagnetic decay of unstable particles, and particles deriving from the decay of hadrons with charm or beauty. Basically, we include any charged particle except those coming from weak decays of strange particles and particles produced in the interaction with the detector material. All associated particles surviving the selection cuts and not matching the adopted criterion are considered as a contamination whose contribution has to be corrected for.

The analysis is performed through the following steps:

1. **D meson selection and signal extraction.** For each single event, "trigger" particles are defined as the selected D meson candidates ($\rm D^0$, $\rm D^+$ and $\rm D^{*+}$) within a given $p_{\rm T}^{\rm trig}$ range. The detection strategy for D mesons at central rapidity is the same as that described in [6] and is based on the reconstruction of decay vertices displayed from the primary vertex by a few hundred μm and on the identification of the decay-particle species. The identification of the charged kaon and pion in the TPC and TOF detectors helps to further reduce the background at low $p_{\rm T}$. An invariant-mass analysis is then used to extract the raw signal yield, using the same fit functions described in [6].

   The D mesons are selected in the rapidity range varying from $|y| < 0.5$ at low $p_{\rm T}$ to $|y| < 0.8$ for $p_{\rm T} > 5$ GeV/c.

2. **Correlation of D candidates with associated tracks.** Particle pairs are formed by associating each trigger particle with the charged primary particles passing the track selection (excluding those coming from the decay of the D-meson candidate) in a specified p_T^{assoc} interval (which can overlap with the $p_{\rm T}^{\rm trig}$ range) and in the pseudo-rapidity range $|\eta| < 0.8$. For D meson candidates in the invariant mass signal region, defined by a $\pm\, 2\sigma$ interval around the D meson mass, the azimuthal angle difference $\phi^{\rm assoc} - \phi^{\rm trigg} \equiv \Delta\phi$ and the pseudorapidity difference $\eta^{\rm assoc} - \eta^{\rm trig} \equiv \Delta\eta$ is evaluated and stored to build two-dimensional correlation distribution.

3. **Subtraction of background correlation from signal distribution.** The invariant mass signal region includes also background D meson candidates. Their contribution to the raw correlation distribution is subtracted as follows. For each $p_{\rm T}$ bin, the mean and the sigma of the invariant mass spectrum are extracted. For $\rm D^0$ and $\rm D^+$, a "background" region is defined in the sidebands of the mass distribution as the interval $4\ GeV/c^2 < |m - m^{\rm pdg}| < 8\ GeV/c^2$. The angular correlation distribution for background candidates in this region is extracted and normalized with respect to the background in the signal region estimated from the mass fit. This normalized background correlation distribution is then subtracted from the raw signal one to obtain the signal correlation distribution. The normalization factor is the ratio of the number of background candidates under the signal peak (obtained bin-counting the candidates in the signal region and subtracting the integral of the fit function for the signal only, in the same range[1]) over the number of background candidates in the sidebands (obtained via bin-counting in the sideband region). This normalized background correlation distribution is then subtracted from the raw signal one to obtain the signal

[1] With this procedure, the statistical fluctuations in the signal region are treated as background fluctuations. This is acceptable, since in most of the $p_{\rm T}$ ranges B > S, hence B fluctuations are higher than S fluctuations.

correlation distribution. In the D^{*+} case candidates in the side bands of the D^0 mass distribution are used to build the background correlation distribution. The normalization factor such as the invariant mass distribution of D^{*+} candidates formed with these candidates matches that of D^{*+} candidates formed with D^0 candidates in the D^0 signal region in the right part of the D^{*+} mass distribution.

4. **Correction for limited acceptance and detector inhomogeneities with Event Mixing** The angular correlation distribution may be affected, even for uncorrelated pair of particles, by structures not due to physical effects, but originating from the limited detector acceptance or from angular inhomogeneities in the trigger and track reconstruction efficiencies as a function of $\Delta\phi$ and $\Delta\eta$. In particular, these always produces an excess of correlations in the near side of the $\Delta\phi$ distribution. Effects of this kind are removed using the Event Mixing technique. In detail, the analysis is executed on the same data sample of the standard one (called "same event" analysis, SE), but the trigger particles found in each event are correlated to charged particles reconstructed in different events ("Mixed Events" analysis, ME).

The differential yield of associated particles per trigger particle is obtained by

$$\frac{1}{N_{\rm trig}}\frac{{\rm d}^2N^{\rm pair}}{{\rm d}\Delta\eta\,{\rm d}\Delta\phi} = B_{ME}(0,0)\times\frac{S(\Delta\eta,\Delta\phi)}{B_{ME}(\Delta\eta,\Delta\phi)}, \tag{1}$$

where $N^{\rm pair}$ is the total number of correlated D-hadron pairs. The functions $S(\Delta\eta,\Delta\phi)$ and $B_{ME}(\Delta\eta,\Delta\phi)$ are the signal and the mixed event background distributions, respectively. The latter is normalized to its value in $(\Delta\eta,\Delta\phi)=(0,0)$ $(B(0,0))$[2]. This kind of normalization, adopted in the analysis of hadron-hadron correlations, relies on the fact that at $(\Delta\eta,\Delta\phi)=(0,0)$ the trigger and associated particle experience the same detector effects. In the D meson case this is true only on average and not at very low $p_{\rm T}$, since D mesons are recontructed from particles that can go in different detector region. However, $(\Delta\eta,\Delta\phi)=(0,0)$ $(B(0,0))$ is in any case the region with maximum efficiency for the pairs (both correlated and uncorrelated). Thus the same convention was adopted.

The signal distribution is the per-trigger-particle yield of pairs found in the same event,

$$S(\Delta\eta,\Delta\phi) = \frac{1}{N_{\rm trig}}\frac{{\rm d}^2N^{\rm same}}{{\rm d}\Delta\eta\,{\rm d}\Delta\phi}, \tag{2}$$

where $N^{\rm same}$ is the number of such pairs within a ($\Delta\eta$,$\Delta\phi$) bin. The background distribution from mixed-event is given by

$$B_{ME}(\Delta\eta,\Delta\phi) = \frac{1}{N_{\rm trig}}\frac{{\rm d}^2N^{\rm mix}}{{\rm d}\Delta\eta\,{\rm d}\Delta\phi}, \tag{3}$$

where $N^{\rm mix}$ denotes the number of mixed-event pairs. The ratio $B(0,0)/B(\Delta\eta,\Delta\phi)$ determines the pair acceptance correction factor. Multiplying the signal distribution by this ratio gives the acceptance-corrected per-trigger-particle associated yield.

5. **Correction for D meson efficiency and associated track efficiency.** After filling the signal and background correlation distributions, it is necessary to take into account also for the correlations with tracks not reconstructed, or not passing the quality selection due to poor reconstruction. Indeed, each pair is weighted by the inverse of the product of the associated track and D meson reconstruction efficiency, ε_{trk} and ε_{trig}. The associated track efficiency dependence on the particle pseudorapidity, transverse momentum, and z-coordinate of the primary vertex is taken into account. For the trigger particle efficiency only the $p_{\rm T}$ and the event multiplicity dependencies of

[2]The $(\Delta\eta,\Delta\phi)=(0,0)$ $(B(0,0))$ value is computed as the average of the bin in the range $-0.2<\Delta\eta<0.2$, $-0.2<\Delta\phi<0.2$.

the efficiency are considered, mainly to avoid large statistical fluctuations on the efficiency values arising when including also the dependency on η, due to the limited size of the Monte Carlo sample from which the D meson efficiencies are evaluated. The details of the efficiency corrections can be found in the following sections. To properly count the number of trigger particles, each D meson is weighted with the inverse of its efficiency in the invariant mass distribution. The main role of the correction for the D meson efficiency is to account for the p_{T} dependence of the correlation distribution within a given D meson p_{T} interval. In fact, only the p_{T} shape of the D meson efficiency is relevant while the average value in the p_{T} range is simplified due to the normalization of the correlation distribution to the number of trigger particles.

6. **Projection in $\Delta\phi$.** The limited statistics available does not allow to study the two dimensional $(\Delta\eta,\Delta\phi)$ distribution, which is therefore projected to the $\Delta\phi$ axis by integrating on $\Delta\eta$¡ 1.

7. **Correction for the contamination of secondary particles** The DCA to primary vertex cut, applied during the associated track selection, has the role of removing the secondary particles from the associated track sample. Secondary particels are indeed produced either from long-lived strange hadrons or from interaction of particles with the detector material. A residual contamination from secondary tracks is hence expected in the correlation distributions. This contamination is estimated from minimum bias Monte Carlo simulation based on Pythia (Perugia?? tune) as described more in detail in the next section. The background-subtracted event-mixing corrected correlations are multiplied by a purity factor to remove this contribution.

8. **Correction for feed-down of D meson from b-hadron decay** The selection strategy employed for the D meson candidates selection enhances the fraction of reconstructed D mesons coming from the decay of a b-hadron. Typical values are of the order of 5% (at low p_{T}) and 20% (at high p_{T}) for the D^0 and the D^+ and smaller than 8% for the D^{*+}. The correlation distribution of these secondary D mesons will be sensitive to the properties of beauty jets and beauty hadron decay, which in general differ from those relative to charm jets and hadrons. The procedure used to subtract this contribution is described in the next section.

9. **Study of correlation properties.** The properties of the azimuthal correlation distribution are quantified by fitting the distribution with a function composed of two Gaussian functions, modelling the near and the away side peaks, and a constant term describing the baseline. The mean of the Gaussian are fixed at $\Delta\phi = 0$ and $\Delta\phi = \pi$. To accomplish the 2π periodicity of the $\Delta\phi$ variable, the Gaussian functions are "duplicated" with mean at $\Delta\phi = 2\pi$ and $\Delta\phi = -\pi$.

   A brief description of the code used in the analysis and various corrections is mentioned in following subsections.

As the difference in the azimuthal angle is periodic ($\Delta\phi = 0 = 2\pi$), the $\Delta\phi$-range is limited to the essential range of 2π. The $\Delta\phi$-limits are chosen to be $[-\pi/2,3\pi/2]$ in order to provide a good visibility of the correlation pattern, which peaks around 0 and π.

3.1 Code used for the analysis

The code used for D meson-hadron correlation analysis is committed to the Ali-Physics. The analysis classes can be found in $ALICE_ROOT/PWGHF/correlationHF/. The D meson specific classes where the aforementioned steps are carried out are AliAnalysisTaskDStarCorrelations, AliAnalysisTaskSED0Correlations and AliAnalysisTaskDplusCorrelations. The classes which are common to the D meson specific analysis which includes the associated particle cuts and the correlation observables are AliHFAssociatedTrackCuts, AliHFCorrelator and AliReducedParticle.

3.2 Corrections

3.2.1 Event Mixing

The event-mixing technique is used for correcting the raw correlation distribution for effects arising from the detector limited acceptance in rapidity and detector spatial inhomogeneities. The calculation of the Event Mixing correlation distribution is performed online.An event pool is created, where events preceding the one containing a D candidate are stored based on their properties (position of the vertex along the z axis and multiplicity). Each time a D meson candidate is found in an event, only the events contained in the same pool as the event under analysis is used to evaluate the correlations for the event mixing correction.

The multiplicity and z vertex position bins for the pools used in the p-Pb analysis are the following:

- Multiplicity bins: $(0,40)\,;(40,65)\,;(65,+\infty)$
- Vertex z (cm) = $(-10,-2.5)\,;(-2.5,2.5)\,;(2.5,10)$

In an ideal case, the mixed event distribution is expected to have a constant flat distribution as function of $\Delta\phi$ and a triangular shaped distribution in $\Delta\eta$ deriving from the limited η acceptance of the detector. The obtained distribution is used as a weight in each correlation bin, i.e, the corrected correlation distribution is calculated as follows:

$$\frac{dN^{corr}(\Delta\phi\Delta\eta)}{d\Delta\phi d\Delta\eta} = \frac{\frac{dN^{SE}(\Delta\phi\Delta\eta)}{d\Delta\phi d\Delta\eta}}{\frac{dN^{ME}(\Delta\phi\Delta\eta)}{d\Delta\phi d\Delta\eta}} \frac{dN^{ME}(0,0)}{d\Delta\phi d\Delta\eta} \tag{4}$$

In the previous equation, the last term stands for the average of the bins in the region $-0.2 < \Delta\eta < 0.2$, $-0.2 < \Delta\phi < 0.2$ (multiple bins are used to minimize the effect of statistical fluctuations on the normalization of the mixed-event plots).

The mixed-event correlation distributions are built in both D meson signal and sideband regions. Both are corrected with the relative distributions. An example of the mixed event distribution is shown in Fig. 1 (middle panels). The expected triangular shape in $\Delta\eta$ addresses the effect of the limited detector pseudo-rapidity acceptance. Note that the mixed-event distribution is limited to the interval $|\Delta\eta| < 1$: the decision to limit the mixed-event correction, and thus the whole analysis, to this range was taken in order to avoid the so-called "wing effect", i.e. the wing-like structures arising in the correlation distribution at large $\Delta\eta$ due to the limited filling of the correlation bins in that region. The event mixing is calculated in the *AliHFCorrelator* class and is computed in the same way for each D meson.

Figure 1: $(\Delta\phi,\Delta\eta)$ correlation in the Sidebands and Signal region from Single Event and Mixing Event analysis for low p_T: $3 < p_T^{\mathrm{D}^+} < 5GeV/c$ with associated track p_T threshold 0.3 GeV/c

Figure 2: $(\Delta\phi,\Delta\eta)$ correlation in the Sidebands and Signal region from Single Event and Mixing Event analysis for mid p_T: $5 < p_T^{\mathrm{D}^+} < 8GeV/c$ with associcated track p_T threshold 0.3 GeV/c

Figure 3: $(\Delta\phi,\Delta\eta)$ correlation in the Sidebands and Signal region from Single Event and Mixing Event analysis for high p_T: $8 < p_T^{\mathrm{D}^+} < 16GeV/c$ with associcated track p_T threshold 0.3 GeV/c

Figures 1, 2, 3 show the 2D correlation in Sideband Region and Signal region from SE and ME analysis for D^+ meson in different p_T region.

3.2.2 *Tracking and D-meson trigger efficiency*

(i) Tracking efficiency is calculated by obtaining the ratio between the yield at the reconstructed level and generated level, for a defined "type" of particles and it is estimated differentially in p_T, η, and z_{vtx} of the event.

Implementation : tracking efficiency maps are produced as TH3D histograms (p_T, η, z_{vtx}) obtained from MC analysis after all event and particles/track selections (summarized in Table. 3). These efficiency maps are used in the analysis tasks to extract single track efficiencies in which each associated track is inserted in correlation plots with a weight of **1/efficiency value**. Example plots of the tracking efficiencies as a function of p_T are shown in Fig. **??** for different particle species. The one-dimension p_T efficiency with different sets of track cuts is almost flat at mid and high p_T range and has small fluctuation in the low p_T region and average efficiency per species in mentioned in Table. 2.

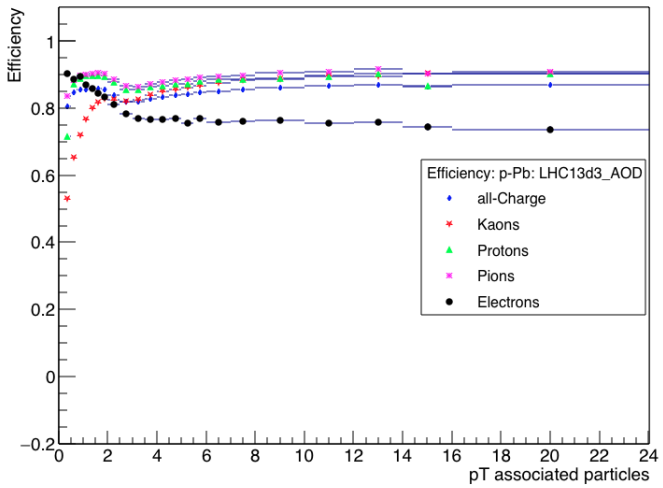

Figure 4: p_T efficiency for different species.

Species / p_t range	**0.3-24.0 GeV/c**	**0.5-24.0 GeV/c**	**0.3-0.5 GeV/c**
all-Charge	0.832211	0.850089	0.804515
Pions	0.865529	0.889492	0.834333
Kaons	0.678151	0.729512	0.528229
Protons	0.853865	0.883295	0.714668
Electrons	0.869452	0.856509	0.903016

Table 2: Average p_T efficiency per species (LHC16q/pass1_woSDD/AOD)

Details of cuts at event level and particle selection at different steps are listed in Table. 3 .

MC Generated		
Event Selection	**Particle Selection**	
	Stages	Cuts
1. -10cm < Zvtx < 10cm	1.MC Part with Generated Cuts	**After Event Selection** Charge PDG Code Physical Primary
2. Multiplicity	2. MC Part with Kine Cuts	**Kinematics Cuts** -0.8<η<0.8 0.3 < pT < 24 (GeV/c)
3. Type of MC process	3. MC Part with Acceptance Cuts	**nhits ref on detectors (ESD only)** a) ITS = 4 b) TPC = 5 c) TOF = 0 d) MOUN = 0
MC Reconstructed		
1. -10cm < Zvtx < 10cm	4. Reco tracks	**After Event Selection** Physical Primary
2. Multiplicity	5. Reco tracks with Kine Cuts	**Kinematics Cuts** -0.8<η<0.8 0 < pT < 24 (GeV/c)
3. Physics Selection	6. MC true with Quality Cuts	**Quality Cuts** SetRequireSigmaToVertex(kFALSE) SetDCAToVertex2D(kFALSE) SetMinNClustersTPC(70) SetMinNClustersITS(3) SetMaxChi2PerClusterTPC(4) SetMaxDCAToVertexZ(1) SetMaxDCAToVertexXY(0.25) SetRequireTPCRet(TRUE) SetRequireITSRet(TRUE) SetClusterRequirementITS(SPD, ..)
	7. Reco tracks with Quality Cuts	**Same as step 6**

Table 3: Single Track Efficiency cuts detail

(ii) D Meson efficiency - Due to limited statistics, the correlation analysis is performed in wide p_T bins and in each of them the reconstruction and selection efficiency of D mesons is not flat (Fig. 5, 6). We correct for the p_T dependence of the trigger efficiency within each p_T-bin. This correction is applied online, by using a map of D meson efficiency as a function of p_T and event multiplicity extracted from MC. While running the analysis, each correlation entry is weighted by **1/trigger efficiency**. It was observed that multiplicity dependence of the efficiency does not bias the extraction of the signal yield from the invariant mass distributions. Efficiency plots for D^+ meson and D^0 meson are shown in Fig. 5 and 6.

Figure 5: Top panel: (p_T, multiplicity) dependence of D^+ meson efficiency. Bottom panels: D^+ meson efficiency in multiplicity for three D^+ $p_T$ranges: 3-5 GeV/c (left), 5-8 GeV/c (center), 8-16 GeV/c (right).

Figure 6: Top panel: (p_T, multiplicity) dependence (left) and p_T dependence (right) of prompt D^0 meson efficiency. Bottom panels: multiplicity dependence of D^0 meson efficiency for three D^0 p_T ranges: 3-4 GeV/c (left), 5-6 GeV/c (center), 8-12 GeV/c (right). For tracklet multiplicity$>$ 120, due to the limited statistics, the efficiency value is fixed to the one obtained for 90$<$tracklet multiplicity$<$120.

3.2.3 Beauty feed-down

The contribution of correlations of D meson from b-hadron decay is subtracted from the uncorrected as:

$$\tilde{C}_{\text{prompt D}}(\Delta\phi) = \frac{1}{f_{\text{prompt}}}\left(\tilde{C}_{\text{inclusive}}(\Delta\phi) - (1-f_{\text{prompt}})\tilde{C}^{\text{MC templ}}_{\text{feed-down}}(\Delta\phi)\right). \quad (5)$$

In the above equation, $\tilde{C}_{\text{inclusive}}(\Delta\phi)$ and $\tilde{C}_{\text{prompt D}}(\Delta\phi)$ are per-trigger azimuthal correlation distributions before and after feed-down contribution subtraction, f_{prompt} is the fraction of prompt D meson and $\tilde{C}^{\text{MC templ}}_{\text{feed-down}}$ is a template of the azimuthal correlation distribution for the feed-down component obtained from Monte Carlo simulation. The value of f_{prompt}, which depends on D-meson species and varies as a function of the p_T, is estimated on the basis of FONLL predictions and using the reconstruction efficiency of prompt and feed-down D mesons, as described in [6]. Typical values ranges from 5 to 20% for the D^0 from low to high p_T and from few percent to **8%** for the D^{*+}. The procedure adopted is the same as what done in pp: however, in p–Pb, in order to consider a possible non-zero v_2-like modulation of the baseline, a range of $0 < v_2 < 0.2$ values for tracks and for secondary D mesons is considered.

4 Systematic uncertainties and checks of analysis consistency

5 Results

Figures 7, 8 and 9 show respectively the results for D^0-h, D^{*+}-h and D^+-h fully corrected azimuthal correlation distributions, on the data sample used in the analysis. Results are shown for $5 < D\ p_{\rm T} < 8$ GeV/c and $8 < D\ p_{\rm T} < 16$ GeV/c, with associated tracks $p_{\rm T} > 0.3$, $p_{\rm T} > 1$ and $0.3 < p_{\rm T} < 1$ GeV/c.

Figure 7: Fully corrected distribution of D^0-hadrons azimuthal correlations, from analysis on the data sample, for the analyzed D^0 $p_{\rm T}$ bins (Column-Left: $5 < {\rm D}^0\ p_{\rm T} < 8$ GeV/c, Column-Right: $8 < {\rm D}^0\ p_{\rm T} < 16$ GeV/c) and associated tracks $p_{\rm T}$ ranges (Row1: >0.3 GeV$/c$, Row2: 0.3 to 1 GeV$/c$, Row3: >1.0 GeV$/c$)

.

Figure 8: Fully corrected distribution of D^+-hadrons azimuthal correlations, from analysis on the data sample, for the analyzed D^+ $p_{\rm T}$ bins (Column-Left: $5 < {\rm D}^+\ p_{\rm T} < 8$ GeV/c, Column-Right: $8 < {\rm D}^+\ p_{\rm T} < 16$ GeV/c) and associated tracks $p_{\rm T}$ ranges (Row1: >0.3 GeV$/c$, Row2: 0.3 to 1 GeV$/c$, Row3: >1.0 GeV$/c$)

.

Figure 9: Fully corrected distribution of D^{*+}-hadrons azimuthal correlations, from analysis on the data sample, for the analyzed D^{*+} $p_{\rm T}$ bins (Column-Left: $5 < {\rm D}^{*+}\ p_{\rm T} < 8$ GeV/c, Column-Right: $8 < {\rm D}^{*+}\ p_{\rm T} < 16$ GeV/c) and associated tracks $p_{\rm T}$ ranges (Row1: >0.3 GeV$/c$, Row2: 0.3 to 1 GeV$/c$, Row3: >1.0 GeV$/c$)

.

Despite being evaluated in the full 2π range, the range of final results was reduced to $[0,\pi]$ radians, reflecting the points outside that range over the value of 0. This allowed to reduce the impact of statistical fluctuations on the data points (supposing equal statistics for a pair of symmetric bins, after the reflection the relative statistical uncertainty for the resulting bin is reduced by a factor $1/\sqrt{2}$). A comparison among reflected distributions and distributions in the full range is shown in Figure **??** (for the average of the three mesons, evaluated as explained in the following paragraph, together with comparison from Monte Carlo simulations).

Correlation distributions are fitted with two Gaussian functions (with means fixed at 0 and π values) + constant, with a periodicity condition applied on the fit (equation 6):

$$f(\Delta\phi) = c + \frac{Y_{NS}}{\sqrt{2\pi}\sigma_{NS}} e^{\frac{(\Delta\phi-\mu_{NS})^2}{2\sigma_{NS}^2}} + \frac{Y_{AS}}{\sqrt{2\pi}\sigma_{AS}} e^{\frac{(\Delta\phi-\mu_{AS})^2}{2\sigma_{AS}^2}} \tag{6}$$

An example of the results from the fit is shown in Figure 5.

5.1 Comparing the three D meson correlation distributions

To check the compatibility of the three D meson analyses, a comparison of the correlation distributions for different D meson and associated track p_T ranges is shown in Figure 10 for the two D-meson kinematic p_T ranges and the two associated track p_T intervals. Though the $\rm D^+$ distributions at high D-meson p_T show an higher baseline with respect to the other mesons, an agreement of the distributions from the three mesons within the uncertainties is found in all the kinematic ranges.

Figure 10: Comparison of $\rm D^0$, $\rm D^+$ and $\rm D^{*+}$-hadron correlation, for the D meson p_T ranges $5 < D\ p_{\rm T} < 8$ GeV/c and $8 < D\ p_{\rm T} < 16$ GeV/c, with associated track transverse momentum in ranges $0.3 < p_T < 1$ GeV$/c$ and $p_T > 1$ GeV$/c$.

5.2 Average of D^0, D^+ and D^{*+} results

Since compatibility within the statistical and systematic uncertainties was found among the D^0, D^+ and D^{*+} azimuthal correlations, and considering that the differences spotted in the correlation distributions observed in Monte Carlo simulations based on Pythia (Perugia-0 tune) are within the statistical uncertainties (though a slight near side hierarchy is present among the three meson results), it was possible to perform a weighted average (eq. 7) of the azimuthal correlation distributions of D^0, D^+ and D^{*+}, in order to reduce the overall uncertainties. The inverse of the sum in quadrature of the statistical uncertainty and of the uncorrelated part of the systematic was used as weight.

$$\left\langle \frac{1}{N_{\rm D}} \frac{dN^{\rm assoc}}{dp_{\rm T}} \right\rangle_{Dmesons} = \frac{\sum_{\rm i=meson} w_i \frac{1}{N_{\rm D}} \frac{dN_i^{\rm assoc}}{d\Delta\phi}}{\sum_{\rm i=meson} w_i} \quad , w_i = \frac{1}{\sigma^2_{i,\rm stat} + \sigma^2_{i,\rm uncorr.syst.}} \tag{7}$$

The statistical uncertainty and the uncertainty on the yield extraction on the average were then recalculated using the formula ($n_{\rm D}$ is the number of mesons considered in the average)

$$\sigma^2 = \frac{1}{n_{\rm D}} \frac{\sum_{\rm i=meson} w_i \sigma_i^2}{\sum_{\rm i=meson} w_i} \tag{8}$$

which, for $\sigma_i^2 = 1/w_i$, coincides with the standard formula giving the uncertainty on a weighted average. The contribution to the average systematic uncertainty for those uncertainty sources not included in the weight definition, was evaluated via error propagation on the formula of the weighted average (7), resulting in equation (9) and (10) for sources considered uncorrelated and correlated among the mesons. In particular, the uncertainties on the associated track reconstruction efficiency, on the contamination from secondary, on the feed-down subtraction, and that resulting from the Monte Carlo closure test were considered fully correlated among the mesons, while those deriving from the yield extraction (included in the weight definition) and on the D meson reconstruction and selection efficiency were treated as uncorrelated.

$$\sigma^2 = \frac{\sum_{\rm i=meson} w_i^2 \sigma_i^2}{\left(\sum_{\rm i=meson} w_i\right)^2} \tag{9}$$

$$\sigma = \frac{\sum_{\rm i=meson} w_i \sigma_i}{\sum_{\rm i=meson} w_i} \tag{10}$$

Figure 11 shows the average of D^0, D^+ and D^{*+} azimuthal correlations with associated tracks with $p_{\rm T} > 0.3$ GeV/c, $p_{\rm T} > 0.5$ GeV/c, $p_{\rm T} > 1$ GeV/c in the D meson $p_{\rm T}$ ranges $3 < p_{\rm T} < 5$ GeV/c, $5 < p_{\rm T} < 8$ GeV/c and $8 < p_{\rm T} < 16$ GeV/c. The fit function is composed of two Gaussian functions with mean fixed at 0 and π and a baseline. The baseline determination is done using the same recipe as used in pp analysis.

Figure 11: Average of D^0, D^+ and D^{*+} azimuthal correlation distributions, in the D meson $p_{\rm T}$ ranges $5 < p_{\rm T} < 8$ GeV/c and $8 < p_{\rm T} < 16$ GeV/c, with associated tracks with $p_{\rm T} > 0.3$ GeV/c, $p_{\rm T} > 1$ GeV/c and $0.3 < p_{\rm T} < 1$ GeV/c.

The usage of weighted average requires, as an underlying assumption, identical results expected for different species (or, at least, compatible within the uncertainties). In case this assumption is not verified, an arithmetic average has to be computed instead, which does not rely on any assumption. As a drawback, the arithmetic average shows higher statistical uncertainties. Anyway, the distributions obtained evaluating the averages with the two approaches were found to be compatible, as shown in Figure **??** for two kinematic cases.

Figure 12: Near side yield for the D-meson average, extracted from fit to the azimuthal correlation distributions, for all the analyzed kinematic ranges. In the right column, for each kinematic region the systematic uncertainties coming from the variation of the fit procedure are shown.

Figure 13: Near side width for the D-meson average, extracted from fit to the azimuthal correlation distributions, for all the analyzed kinematic ranges. In the right column, for each kinematic region the systematic uncertainties coming from the variation of the fit procedure are shown.

Figure 14: Height of the baseline for the D-meson average, extracted from fit to the azimuthal correlation distributions, for all the analyzed kinematic ranges. In the right column, for each kinematic region the systematic uncertainties coming from the variation of the fit procedure are shown.

5.3 Nearside associated yield, nearside width and baseline as function of the D meson p_T

The extraction of the parameters (i.e. near side associated yield, near side width, and baseline) is performed using the strategy described above. The pedestal is calculated as the weighted average of the 8 points (for the full 2π range plots) lying in the so-called "transverse region", i.e. the interval $\frac{\pi}{4} < |\Delta\phi| < \frac{\pi}{2}$.

The evaluation of the systematics is performed as follows:

- The maximum variation of the parameters between the systematics from the fitting procedure (variation of the method to fix the pedestal) and the variation obtained by shifting the points in $\Delta\phi$ within the uncorrelated systematic band
- For the estimation of the baseline and of the near side associated yield, that value is added in quadrature with the correlated systematics in the correlation plot. In case of the near side width this is not the case, since it is not affected by the different normalization

$$\sigma^{syst} = \sqrt{\left(Max\left(\Delta par^{ped.mode}, \Delta par^{\Delta point}\right)\right)^2 + \left(\sigma^{corr}_{Syst}\right)^2} \tag{11}$$

5.3.1 Results for near-side yield, near-side width and baseline

Figures 12, 13 and 14 present the near-side associated yield, width (the sigma of the Gaussian part of the fit functions) and the height of the baseline, for the average correlation distributions, in the kinematic ranges studied in the analysis. For each kinematic range, the correspondent plot showing the systematic uncertainty of the considered observable from the variation of the fit procedure (which is not the full uncertainty) is presented as well.

6 Conclusions

7 Bibliography

References

[1] J. Adam et al. [ALICE Collaboration], Nature Physics (2017) doi:10.1038/nphys4111.

[2] [E791 Collaboration],Correlations between D and $\bar{D}$ mesons produced in 500GeV π -nucleon interactions; EPJdirect C1 (2008)

[3] [CDF Collaboration], Measurement of Charm Meson pair Cross Section; CDF-Note 8621 2006.

[4] X.Zhu, N.Xu, P.Zhuang, Phys.Rev.Lett.100:152301,2008, arXiv:0709.0157.

[5] M. Nahrgang, J. Aichelin, P. B. Gossiaux, K. Werner, arXiv:1305.3823.

[6] B. Abelev et al. [ALICE Collaboration], JHEP **01** (2012) 128.